

Received November 7, 2019, accepted November 20, 2019, date of publication November 26, 2019, date of current version March 2, 2020.

Digital Object Identifier 10.1109/ACCESS.2019.2955968

Application of the Non-Local Log-Euclidean Mean to Radar Target Detection in NonHomogeneous Sea Clutter

WEI CHEN^{ID}¹ AND SIYU CHEN^{ID}²

¹Industrial Center, Nanjing Institute of Technology, Nanjing 211167, China

²Department of Electrical and Computer Engineering, Technical University of Munich, D-80333 Munich, Germany

Corresponding author: Siyu Chen (siyu_chen123@126.com)

ABSTRACT In order to effectively detect moving targets in a nonhomogeneous sea clutter, the non-local Log-Euclidean mean is studied and an effective algorithm based on non-local Log-Euclidean mean is proposed. Firstly, the mathematical model of the received signal returned from a target is established. Then, the Log-Euclidean distance is introduced and the non-local method is employed for computing the Log-Euclidean mean. Furthermore, an adaptive matched filter with non-local Log-Euclidean mean is investigated. As the non-local method adopts samples similar to a given sample to estimate the Log-Euclidean mean, a robust covariance matrix estimation is obtained in a nonhomogeneous sea clutter. In the end, numerical simulations and real High-Frequency radar datasets are used to verify the validity of this proposed algorithm, and the results demonstrate that the proposed method not only outperforms the conventional detection method but also exhibits more robustness in a nonhomogeneous environment.

INDEX TERMS Covariance matrix estimation, Log-Euclidean distance, target detection, non-local mean, nonhomogeneous sea clutter.

I. INTRODUCTION

Robust and effective detection of a moving target embedded in a nonhomogeneous sea clutter in a High-Frequency (HF) radar system is one of the fundamental problems in both military and civil remote sensing fields. Due to the variation of sea states (wind speed, wave height), and parameters of the system (grazing angle, polarization), sea clutter usually shows significant nonhomogeneous in an HF system [1]. The nonhomogeneous sea clutter often contains the so-called outliers caused by clutter edge, sea spike, and other target which is not interested in the processing. Outliers that have different spectral properties with others have an impact on the clutter covariance estimation, which may result in poor detection performance [2]–[4]. As a consequence, it is necessary and important to improve the detection performance of an HF system.

A lot of efforts have been made to improve the detection performance of an HF system, classical detection methods, such as Kelly's detector [5], adaptive matched filter (AMF) [6], [7], have achieved well performance in a

homogeneous environment. However, the estimation accuracy of sample covariance matrix is strongly affected by the nonhomogeneous property of samples data. When detecting signals buried in a nonhomogeneous sea clutter, severe performance degradations are experienced. To ameliorate the detection performance, many works are concentrated on incorporating the knowledge-aided paradigm into the detector design. For instance, Maio *et al.* [8] achieves significant performance improvements by incorporating the geographic information of surrounding environment into detector design. In [9], the authors suppose that the clutter data obeys a suitable distribution. Based on this clutter model, the Bayesian approach is exploited to obtain a Generalized Likelihood Ratio Test (GLRT) detector. Real data is used to analyze the detection performance, and the results validate the superiority of the proposed detector. In [10]–[13], the clutter is modeled as a auto-regressive process, and the structural information on clutter covariance matrix is used to be estimated. However, these detection methods, which achieve performance improvements, depend on the prior knowledge of clutter distribution [14], [15].

Another popular technique is the geometry-based detection method proposed by Barbaresco [16], [17], and

The associate editor coordinating the review of this manuscript and approving it for publication was Chengpeng Hao^{ID}.

Hua *et al.* [18], [19], where clutter data is modeled as a Hermitian positive-definite (HPD) matrix, which represents the clutter correlation characteristics or clutter power. Geometry-based detection methods have been applied for wake turbulence monitoring [20], [21], and the superiority has been validated by real data with respect to traditional methods. In [16], [22], the Riemannian mean and median are used together with the geometric detection framework, and results on target detection in coastal X-band and HF system have shown the performance improvement compared to the classical fast Fourier transform (FFT) based constant false alarm rate (CFAR) detector. In [23], space-time adaptive processing (STAP) with a Riemannian mean estimator has achieved significant improvement. Moreover, information divergence measures are presented and applied to target detection. In [19], five geometric measures-based detectors are proposed, and numerical experiments on simulation data and real radar data are given to validate the superiority. Significant signal-to-noise/clutter ratio (SNR/SCR) improvement is achieved via geometric measures in an HF system. Geometric means have also been employed to select training sample data in nonhomogeneous environment.

The mean associated with the Euclidean distance is not robust to the outlier. Then, the performance of Euclidean mean-based covariance estimator is poor, which results in a remarkably degradation in detection performance in nonhomogeneous clutter. Recently, many works have proven that the mean associated with the Log-Euclidean distance has perfect robustness, and can achieve an accurate and stable estimation performance in nonhomogeneous clutter [24]–[26]. Following this guideline, in this paper, we propose a non-local Log-Euclidean mean of HPD matrices by incorporating a non-local method into the computation of Log-Euclidean mean in nonhomogeneous clutter. In particular, the Log-Euclidean mean-based sample selection algorithm is utilized to eliminate the outlier in nonhomogeneous clutter. Similar sample data is selected via clutter statistical characteristics in the non-local domain of cell under test (CUT). Then, the selected homogeneous sample data in each cell is modeled as an HPD matrix. These HPD matrices estimated by the sample data in the non-local domain are used to compute the Log-Euclidean mean, that is the non-local Log-Euclidean mean. Furthermore, an AMF with the non-local Log-Euclidean mean estimator is designed and applied to target detection in nonhomogeneous clutter in an HF system. The output SNR/SCR and the robustness to outlier are analyzed, and numerical experiments and real HF clutter data are given to validate the superiority of the proposed algorithm with respect to its traditional ones.

The remainder of this paper is organized as follows. In Section 2, the mathematical model of the received echo signal is presented. Section 3 introduces the non-local sample data selection method. Particularly, the Log-Euclidean mean is used together with the generalized inner product (GIP) algorithm to eliminate outliers in the nonhomogeneous clutter. The non-local Log-Euclidean mean-based

AMF algorithm is proposed in Section 4. Then, some experiments on real sea clutter datasets are used for verification in Section 5. Finally, some concluding remarks are given in Section 6.

A. NOTATION

In this paper, a boldface lower-case letter \mathbf{a} denotes a vector, and a boldface upper-case letter \mathbf{A} denotes a matrix. Symbol \mathbf{A}^H represents the conjugate transpose of matrix \mathbf{A} . $1j$ is the imaginary unit, i.e., $\sqrt{-1} = 1j$. The $n \times n$ identity matrix is denoted by \mathbf{I}_n . All $n \times n$ Hermitian matrices are represented as $\mathbb{H}(n)$. $\mathbb{P}(n)$ stands for the set of $n \times n$ Hermitian positive-definite matrices. \mathbb{R} is the set of real numbers. Symbols $\det(\cdot)$ and $\text{tr}(\cdot)$ denote the determinant and the trace of a matrix, respectively. $a!$ denotes the factorial of a . Symbol $\|\mathbf{A}\|_F$ denotes the Frobenius norm of matrix \mathbf{A} . The matrix logarithm and matrix exponent of a positive-definite matrix \mathbf{A} are noted by $\log(\mathbf{A})$ and $\exp(\mathbf{A})$, respectively.

II. THE MATHEMATICAL MODEL OF RECEIVED SIGNAL

In this Section, the mathematical model of echo signal is presented. Consider N -channel linear array, and the space of each sensor is d . The length of carrier wave is λ , and the number of pulses in each cell in one coherent processing interval (CPI) is M . The received signal in the i -th cell can be expressed as

$$\mathbf{x}_i = \alpha_i \mathbf{s}(f, \theta) + \mathbf{c}_i + \mathbf{n}_i \quad (1)$$

where θ is the phase angle. α_i denotes the amplitude of echo signal, and f is the normalized Doppler frequency. \mathbf{c}_i and \mathbf{n}_i stand for the clutter and the electrical noise, respectively. The steer vector $\mathbf{s}(f, \theta)$ is constituted by the space and temporal components,

$$\mathbf{s}(f, \theta) = \mathbf{s}_{tem}(f) \otimes \mathbf{s}_{spa}(\theta) \quad (2)$$

where $\mathbf{s}_{tem}(f)$ denotes the temporal component, and $\mathbf{s}_{spa}(\theta)$ is the space component. \otimes stands for the Kronecker product. $\mathbf{s}_{tem}(f)$ and $\mathbf{s}_{spa}(\theta)$ are formulated as,

$$\mathbf{s}_{tem}(f) = [1 \quad \exp(j2\pi f) \quad \dots \quad \exp(j2\pi(M-1)f)]^T \quad (3)$$

$$\mathbf{s}_{spa}(\theta) = [1 \quad \exp(j2\pi d \sin(\theta)/\lambda) \quad \dots \quad \exp(j2\pi d(N-1) \sin(\theta)/\lambda)]^T \quad (4)$$

According to the mentioned mathematical model of echo signal, a non-local sample selection algorithm is used to eliminate the nonhomogeneous clutter data.

III. NON-LOCAL SAMPLE DATA SELECTION

In this Section, a non-local sample selection method is introduced. Firstly, the pulse data in each cell is modeled as an HPD matrix, and the non-local domain is obtained via the Log-Euclidean distance between two HPD matrices. Then, the Log-Euclidean mean is used together with the GIP algorithm to eliminate outliers in the non-local domain.

A. FORMULATION OF NON-LOCAL DOMAIN

The pulse data contains the power information and the correlation information. Given a n -length pulses data $\mathbf{x} = [x_1, x_2, \dots, x_n]^T$, \mathbf{x} can be modeled as a covariance matrix \mathbf{R} ,

$$\mathbf{R} = \mathbf{x}\mathbf{x}^H \tag{5}$$

where covariance matrix \mathbf{R} is Hermitian but not positive-definite. HPD matrix has many attractive properties, and is the most studied example in the last decades. In order to facilitate the analysis, covariance matrix \mathbf{R} can be transformed to an HPD matrix \mathbf{P} as follow,

$$\mathbf{P} = \mathbf{R} + \mathbf{I}_n \tag{6}$$

All $n \times n$ HPD matrices form the space $\mathbb{P}(n)$. Given two HPD matrices \mathbf{P}_1 and \mathbf{P}_2 in $\mathbb{P}(n)$, the Log-Euclidean distance between them can be formulated as,

$$d_{LogE}(\mathbf{P}_1, \mathbf{P}_2) = \|\log(\mathbf{P}_1) - \log(\mathbf{P}_2)\|_F \tag{7}$$

The Log-Euclidean distance is defined in the tangent space on $\mathbb{P}(n)$. Matrix logarithm maps a point on $\mathbb{P}(n)$ into its tangent space, while matrix exponent maps a point on its tangent space into $\mathbb{P}(n)$.

Consider a real number y and a set of m real numbers $\{y_1, y_2, \dots, y_m\}$, the distance between y and y_1 can be defined as,

$$d(y, y_1) = |y - y_1| \tag{8}$$

Compute m distances $|y - y_1|, |y - y_2|, \dots, |y - y_m|$ and sort them in increasing order. Then, real numbers according to the first K distances constitute the non-local domain $\{y_1, y_2, \dots, y_K\}$ of y .

Similarly, given an HPD matrix \mathbf{P}_D in CUT and its surrounding matrices $\{\mathbf{P}_1, \mathbf{P}_2, \dots, \mathbf{P}_m\}$, m Log-Euclidean distances $d_{LogE}(\mathbf{P}, \mathbf{P}_1), d_{LogE}(\mathbf{P}, \mathbf{P}_2), \dots, d_{LogE}(\mathbf{P}, \mathbf{P}_m)$ are computed and sorted in increasing order. A set of K HPD matrices $\{\mathbf{P}_1, \mathbf{P}_2, \dots, \mathbf{P}_K\}$ with respect to the first K Log-Euclidean distances constitute the non-local domain of CUT. The HPD matrices in this domain have some similar structures to \mathbf{P}_D , such as eigenvalues.

B. NON-LOCAL LOG-EUCLIDEAN MEAN-BASED SAMPLE SELECTION

In a nonhomogeneous clutter environment, the outlier may have an effect on the estimation accuracy of the clutter covariance matrix, which can result in poor detection performance. Consequently, it is necessary to select homogeneous sample to estimate the clutter covariance matrix. A. Aubry has exploited the GIP algorithm together with geometric barycenters to discard outliers in nonhomogeneous sample data [25]. In compound Gaussian clutter, the clutter covariance matrix is estimated using the sample data censored from the non-homogeneous clutter to improve the detection performance of a normalized adaptive matched filter [26]. In this subsection, the GIP algorithm is used together with the non-local Log-Euclidean mean to select homogeneous sample data.

As mentioned above, given an HPD matrix \mathbf{P}_D , its corresponding non-local domain $\{\mathbf{P}_1, \mathbf{P}_2, \dots, \mathbf{P}_K\}$ can be obtained. Then, the Log-Euclidean mean in this non-local domain is the solution of minimization problem as blow,

$$\min_{\mathbf{P} \in \mathbb{P}(n)} \sum_{i=1}^{i=K} d_{LogE}^2(\mathbf{P}, \mathbf{P}_i) \tag{9}$$

Substitute Eq.(7) into Eq.(9), and the minimization problem can be written as,

$$\min_{\mathbf{P} \in \mathbb{P}(n)} \sum_{i=1}^{i=K} \|\log(\mathbf{P}) - \log(\mathbf{P}_i)\|_F^2 \tag{10}$$

Let $F(\mathbf{P})$ denotes the function,

$$F(\mathbf{P}) = \sum_{i=1}^{i=K} \|\log(\mathbf{P}) - \log(\mathbf{P}_i)\|_F^2 \tag{11}$$

Then, the derivative of $F(\mathbf{P})$ is given as,

$$\Delta F(\mathbf{P}) = 2 \sum_{i=1}^{i=K} (\log(\mathbf{P}) - \log(\mathbf{P}_i))\mathbf{P}^{-1} \tag{12}$$

Let Eq.(12) equals to zero, and we can obtain,

$$\frac{1}{K} \sum_{i=1}^{i=K} \log(\mathbf{P}_i) = \log(\mathbf{P}) \tag{13}$$

According to Eq.(13), the solution of the minimization problem Eq.(10) is given as,

$$\mathbf{P} = \exp\left\{\frac{1}{K} \sum_{i=1}^{i=K} \log \mathbf{P}_i\right\} \tag{14}$$

where \mathbf{P} is the non-local Log-Euclidean mean, and is also an HPD matrix.

The robustness of Log-Euclidean mean outperforms that of Euclidean mean which is used in the GIP sample selector. Here, the influence function [24] is employed to analyze the robustness of Log-Euclidean mean. Suppose $\tilde{\mathbf{P}}$ be the Log-Euclidean mean of m HPD matrices $\{\mathbf{P}_1, \mathbf{P}_2, \dots, \mathbf{P}_m\}$. $\tilde{\mathbf{P}}$ is the Log-Euclidean mean of m HPD matrices and n outliers $\{\mathbf{Q}_1, \mathbf{Q}_2, \dots, \mathbf{Q}_n\}$ with a weight $\varepsilon (\varepsilon \ll 1)$. Then, a relation between $\tilde{\mathbf{P}}$ and $\tilde{\tilde{\mathbf{P}}}$ can be given as,

$$\tilde{\tilde{\mathbf{P}}} = \tilde{\mathbf{P}} + H(\mathbf{Q}) \tag{15}$$

where $H(\mathbf{Q})$ is the influence function of Log-Euclidean mean. The influence function can be formulated as $H(\mathbf{Q}) = \tilde{\tilde{\mathbf{P}}} - \tilde{\mathbf{P}}$. That is to say, the influence function elaborates the difference between the Log-Euclidean mean $\tilde{\mathbf{P}}$ of HPD matrices and the Log-Euclidean mean $\tilde{\tilde{\mathbf{P}}}$ of HPD matrices and the injected outliers. It is obvious that a smaller value of influence function means a smaller difference between $\tilde{\mathbf{P}}$ and $\tilde{\tilde{\mathbf{P}}}$. As $\tilde{\mathbf{P}}$ is the Log-Euclidean mean of HPD matrices and the injected outliers, a smaller difference between $\tilde{\mathbf{P}}$ and $\tilde{\tilde{\mathbf{P}}}$ means a smaller influence of outliers on the Log-Euclidean mean. The robustness of the Log-Euclidean mean indicates the influence

of outliers on the mean. Thus, it can be concluded that a smaller influence function means better robustness.

Proposition 1: The influence function of Log-Euclidean mean related to the Log-Euclidean distance, of m HPD matrices $\{\mathbf{P}_1, \mathbf{P}_2, \dots, \mathbf{P}_m\}$ and n outliers $\{\mathbf{Q}_1, \mathbf{Q}_2, \dots, \mathbf{Q}_n\}$ is given by,

$$H(\mathbf{Q}) = \frac{1}{n} \sum_{j=1}^n (\log(\mathbf{Q}_j) - \log(\bar{\mathbf{P}})) \bar{\mathbf{P}} \quad (16)$$

The detailed proof can be seen in Appendix.

Proposition 2: The influence function of Euclidean mean related to the Euclidean distance, of m HPD matrices $\{\mathbf{P}_1, \mathbf{P}_2, \dots, \mathbf{P}_m\}$ and n outliers $\{\mathbf{Q}_1, \mathbf{Q}_2, \dots, \mathbf{Q}_n\}$ is given by,

$$H(\mathbf{Q}) = \frac{1}{n} \sum_{j=1}^n (\mathbf{Q}_j - \bar{\mathbf{P}}) \quad (17)$$

The detailed proof also can be seen in Appendix.

Based on the influence function, the robustness of Euclidean mean and Log-Euclidean mean can be analyzed quantitatively. This work will be done in Section 5. As satisfactory performances are achieved when the sample data share the same spectral property, the outliers contained in the nonhomogeneous sample data must be discarded. However, the homogeneity spectral property could not hold, because of the presence of outliers within the sample data in nonhomogeneous clutter. A sample selector is necessary to choose the homogeneous data used in the covariance matrix estimation. According to the Log-Euclidean distance and its corresponding Log-Euclidean mean, the sample data selection strategy can be given as,

- 1) Compute the HPD matrix $\mathbf{P}_i, i = 1, 2, \dots, m$ using the sample data in each cell, as Eq.(6);
- 2) Given the HPD matrix \mathbf{P}_D , calculate m Log-Euclidean distances $d_{LogE}(\mathbf{P}_D, \mathbf{P}_i), i = 1, 2, \dots, m$. Sort these distances in increasing order, and the first K distances constitute the non-local domain of \mathbf{P}_D ;
- 3) The Log-Euclidean mean estimator $\hat{\mathbf{P}}$ is achieved using the sample data of non-local domain, as Eq.(14);
- 4) For all the sample data in the non-local domain, compute the GIP

$$\beta_i = \mathbf{x}_i^H \hat{\mathbf{P}}^{-1} \mathbf{x}_i, \quad i = 1, 2, \dots, K \quad (18)$$

and sort β_i in decreasing order;

- 5) The sample data with large value β_i is treated as the outlier and is discarded.

Based on the sample data selection strategy, we can obtain the most homogeneous sample data. Then, accurate Log-Euclidean estimator is achieved, which is estimated using the selected homogeneous sample.

IV. NON-LOCAL LOG-EUCLIDEAN MEAN-BASED TARGET DETECTION ALGORITHM

In this Section, the problem of target detection is formulated, and then a non-local Log-Euclidean mean-based target detection algorithm is presented.

Consider a detection problem, which can be given as,

$$\begin{cases} H_0 : \begin{cases} \mathbf{x} = \mathbf{n} + \mathbf{c} \\ \mathbf{x}_i = \mathbf{n}_i + \mathbf{c}_i, i = 1, 2, \dots, K \end{cases} \\ H_1 : \begin{cases} \mathbf{x} = \beta \mathbf{s} + \mathbf{n} + \mathbf{c} \\ \mathbf{x}_i = \mathbf{n}_i + \mathbf{c}_i, i = 1, 2, \dots, K \end{cases} \end{cases} \quad (19)$$

where H_0 and H_1 denote the hypotheses of the absence and presence of a target. K is the number of sample data which are censored from the nonhomogeneous sample data in non-local domain. \mathbf{x} , \mathbf{c} , and \mathbf{n} are the received signal, clutter data, and white noise, respectively. The terms \mathbf{c} and \mathbf{c}_i are the compound Gaussian vectors, and can be formulated as,

$$\mathbf{c} = \sqrt{\tau} \mathbf{g}, \quad \mathbf{c}_i = \sqrt{\tau_i} \mathbf{g}_i, \quad i = 1, 2, \dots, K \quad (20)$$

where \mathbf{g} and \mathbf{g}_i both are N -dimensional zero-mean Gaussian vectors, and share the same covariance matrix Σ ,

$$\Sigma = \sigma_c^2 \rho^{|i-k|} e^{2\pi f(i-k)} + \mathbf{I}, \quad i, k = 1, 2, \dots, N \quad (21)$$

where σ_c^2 denotes the clutter-to-noise ratio, and ρ is the one-lag correlation coefficient. τ and τ_i are the independent and identical distribution real random variables, particularly, they are supposed to follow the inverse gamma distribution,

$$f(z) = \frac{\beta^\alpha}{\Gamma(\alpha)} z^{-\alpha-1} \exp(-\frac{\beta}{z}), \quad z \geq 0 \quad (22)$$

where β and α denote the scale and shape parameters, respectively. $\Gamma(\cdot)$ is the gamma function.

The adaptive matched filter is usually used for target detection in an HF system, and the scheme can be given as,

$$\frac{\mathbf{s}^H \hat{\Sigma}^{-1} \mathbf{x}}{(\mathbf{s}^H \hat{\Sigma}^{-1} \mathbf{s})} \underset{H_1}{\overset{H_0}{\gtrless}} \gamma \quad (23)$$

where $\hat{\Sigma}$ denotes the estimated clutter covariance matrix. γ is the threshold derived by the Monte Carlo method. Given a probability of false alarm (P_{fa}), the appropriate threshold can be given as,

$$\gamma = \frac{K+1}{K-N+1} [(P_{fa})^{(-\frac{1}{K-N+2})} - 1] \quad (24)$$

More details of the proof can be seen in Appendix.

Given an HPD matrix \mathbf{P}_0 , its surrounding M HPD matrices are $\{\mathbf{P}_1, \mathbf{P}_2, \dots, \mathbf{P}_M\}$, and then, its non-local domain $\{\mathbf{P}_1, \mathbf{P}_2, \dots, \mathbf{P}_{K_0}\}$ can be obtained according to the method presented in Section III-A. The Log-Euclidean mean can be computed using K_0 HPD matrices in the non-local domain. To discard outliers in the non-local domain, the GIP algorithm is used together with the Log-Euclidean mean to choose the most homogeneous sample data $\{\mathbf{P}_1, \mathbf{P}_2, \dots, \mathbf{P}_K\}$. The clutter covariance matrix $\hat{\Sigma}$ can be estimated using the K homogeneous sample data, and the AMF algorithm with the estimated covariance matrix $\hat{\Sigma}$ is applied for target detection embedded in sea clutter in next context. The computational cost is relative expensive, as the algorithm involves several operations of matrix exponent, logarithm and inverse.

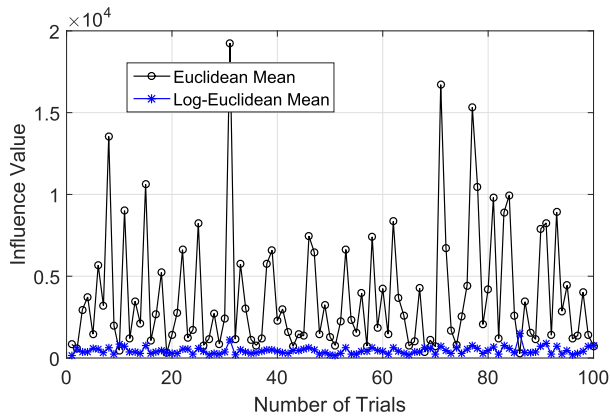


FIGURE 1. Influence function values of 100 trials. $M = 20, N = 8, N_{outlier} = 1$.

V. EXPERIMENTAL RESULTS

Many covariance matrix estimators have been used for sample data selection and target detection in nonhomogeneous clutter, e.g., Log-Euclidean mean, root-Euclidean mean, power-Euclidean mean, cholesky mean, and Euclidean mean. It has been proven in [25], [26] that the Log-Euclidean mean estimator has the best sample selection performance among these means, and the AMF with the Log-Euclidean mean has the best detection performance among their corresponding algorithms. In this Section, the performance of our proposed algorithm is analyzed via numerical experiments in comparison with the AMF with the classical covariance matrix estimator. Firstly, the robustness of the Log-Euclidean mean is analyzed in a nonhomogeneous clutter; and then, the correct selection rate of the non-local Log-Euclidean mean-based sample selector is given in comparison with the conventional method; finally, real clutter data are given to validate the superiority of the proposed algorithm.

A. ROBUSTNESS ANALYSIS

To analyze the robustness of the Log-Euclidean mean in a nonhomogeneous clutter, sample data with numbers of injected outliers are simulated. m sample data treated as homogeneous data are generated from a zero-mean multidimensional Gaussian distribution with a covariance matrix given as Eq.(21). The clutter-to-noise ratio is $\sigma_c^2 = 15 \text{ dB}$, and the one-lag correlation coefficient is $\rho = 0.92$. The clutter normalized Doppler frequency is $f = 0.25$. n outliers are obtained by adding a signal $\mathbf{s} = \alpha[1, e^{j2\pi f_{outlier}}, \dots, e^{j2\pi(l-1)f_{outlier}}]$ into n homogeneous sample data, where α denotes the amplitude value. In the simulation, the normalized Doppler frequency is $f_{outlier} = 0.2$, and the dimension of sample data is $l = 8$. 20 homogeneous sample data is used for computing the Log-Euclidean mean, and the influence function value is obtained by adding a outlier into the homogeneous sample data. Plots of 100 trials are given in Figure 1.

It can be noted from Figure 1 that the influence function value of Euclidean mean is larger than that of Log-Euclidean mean. This means that the influence of outliers on the

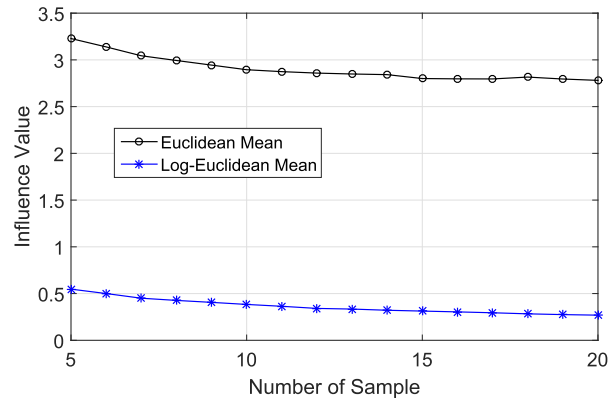


FIGURE 2. Influence function values under different numbers of sample data. M varies from 5 to 20, $N = 8, N_{outlier} = 1$.

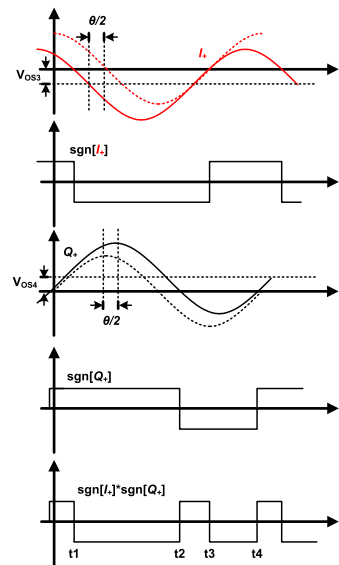


FIGURE 3. Influence function values under different numbers of outliers. $M = 20, N = 8, N_{outlier}$ varies from 1 to 15.

Log-Euclidean mean is smaller than on the Euclidean mean. It can be concluded that the Log-Euclidean mean is more robust than the Euclidean mean when the sample data contains an outlier. To make further efforts to verify the robustness, the influence of outliers on different numbers of sample is analyzed. The number of outlier is $n = 1$, and the number of sample data varies from 5 to 20. The influence function values are shown in Figure 2.

From Figure 2 we can know that the influence function value decreases when the number of sample data increases. This implies that the influence of outlier on the Euclidean mean and the Log-Euclidean mean become smaller with increasing numbers of sample data. Moreover, the influence function value of the Euclidean mean is larger than that of the Log-Euclidean mean under different numbers of sample data. These results suggest that the Log-Euclidean mean is more robust than the Euclidean mean with different numbers of sample data.

In order to analyze the influence of different numbers of outliers on the Euclidean mean and the Log-Euclidean mean,

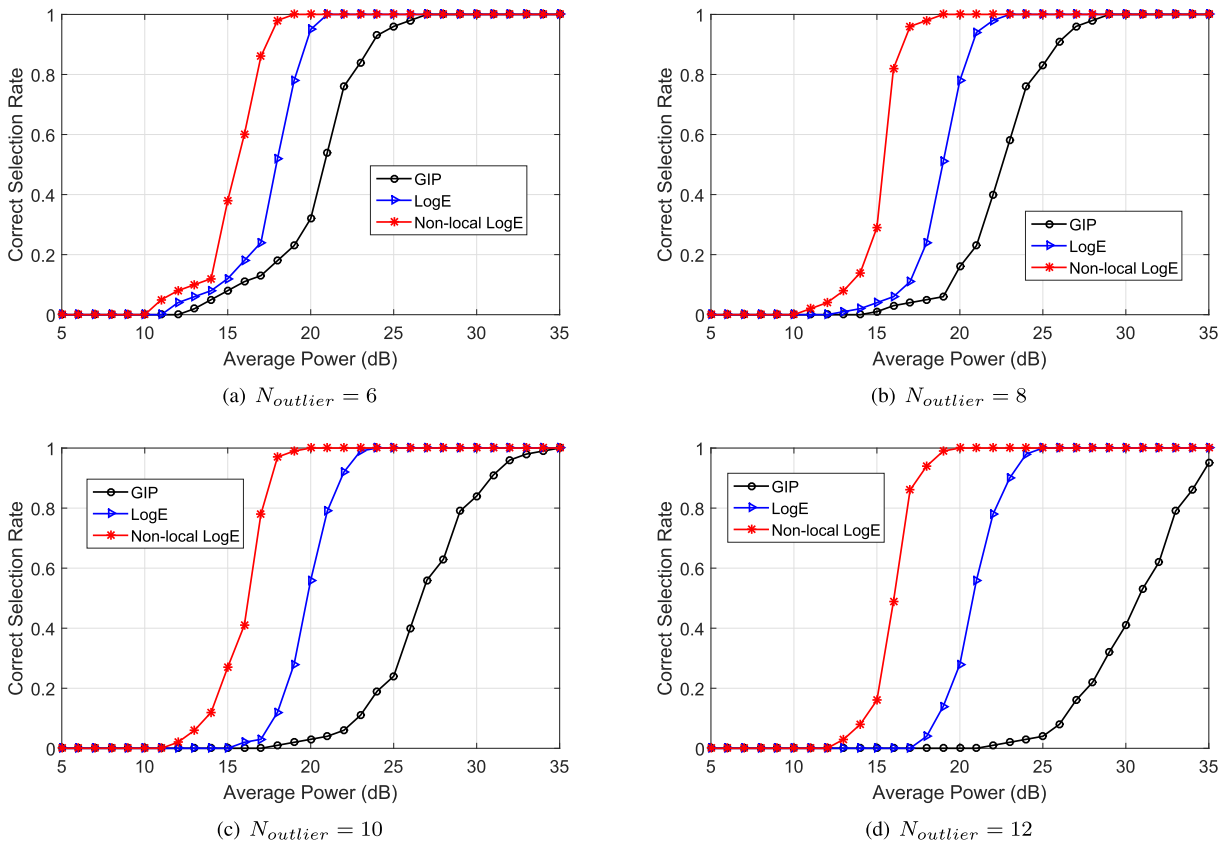


FIGURE 4. Illustrating the correct selection rate against average power from 5 dB to 35 dB with different numbers of outliers. $M = 100$, $N = 8$, $\sigma_c^2 = 15$ dB, $\rho = 0.92$, $f = 0.25$.

the influence function values with numbers of outliers are computed. The number of sample data is $m = 20$, and the dimension of sample data is $N = 8$. The number of outlier varies from 1 to 15. The influence function values of different numbers of outliers are illustrated in Figure 3.

From Figure 3, we can find that the influence values of different numbers of outliers on the Euclidean mean and the Log-Euclidean mean are not very large. It means that the number of outlier has little effect on the estimation accuracy of the Euclidean mean and the Log-Euclidean mean. Furthermore, the influence of different numbers of outliers is larger on the Euclidean mean than on the Log-Euclidean mean. These results demonstrate that the Log-Euclidean mean is more robust than the Euclidean mean.

In this paper, the three algorithms, including the AMF with the Euclidean mean, the AMF with the Log-Euclidean mean, and the AMF with the non-local Log-Euclidean mean, are provided to compare the detection performance. However, the Log-Euclidean mean is used both in the AMF with the Log-Euclidean mean, and the AMF with the non-local Log-Euclidean mean. Thus, only to compare the robustness of the Euclidean mean and the Log-Euclidean mean.

B. PERFORMANCE ANALYSIS OF THE SAMPLE SELECTOR

The real environment is simulated to evaluate the correct selection rate of non-local Log-Euclidean mean estimator in comparison with the GIP and Log-Euclidean mean estimator.

The total secondary sample data is set to be $M = 100$, and the dimension of sample data in each cell is $N = 8$. The clutter-to-noise ratio is $\sigma_c^2 = 15$ dB, and the one-lag correlation coefficient is $\rho = 0.92$. The clutter normalized Doppler frequency is $f = 0.25$. The correct selection rate denotes the proportion of the selected outliers to the selected sample. For instance, 8 outliers are injected into the 100 secondary samples. The GIP of each sample is computed as (18), and all values of GIP are sorted in decreasing order. Sample data corresponding to the first 8 values are selected. When there are 4 outliers in the selected 8 samples, the correct selection rate is 0.5. In the simulation, The Monte Carlo simulation is repeated 500 times to compute the relative frequency of correct selection rate. Several outliers are injected into the clutter data, and each outlier has the same power. The normalized Doppler frequency of the outlier is set to be 0.2. Figure 4 gives plots of correct selection rate against average power under different numbers of outliers from 6 to 12 with an interval of 2.

It can be observed from Figure 4 that both the Log-Euclidean and non-local Log-Euclidean selectors have better performance than the GIP selector. Particularly, the non-local Log-Euclidean selector have the highest correct selection rate. It is well known that the performance of covariance estimator decreases in heterogeneous clutter. The selection performance of the GIP with mean estimator is related with the robustness of mean. According to the results

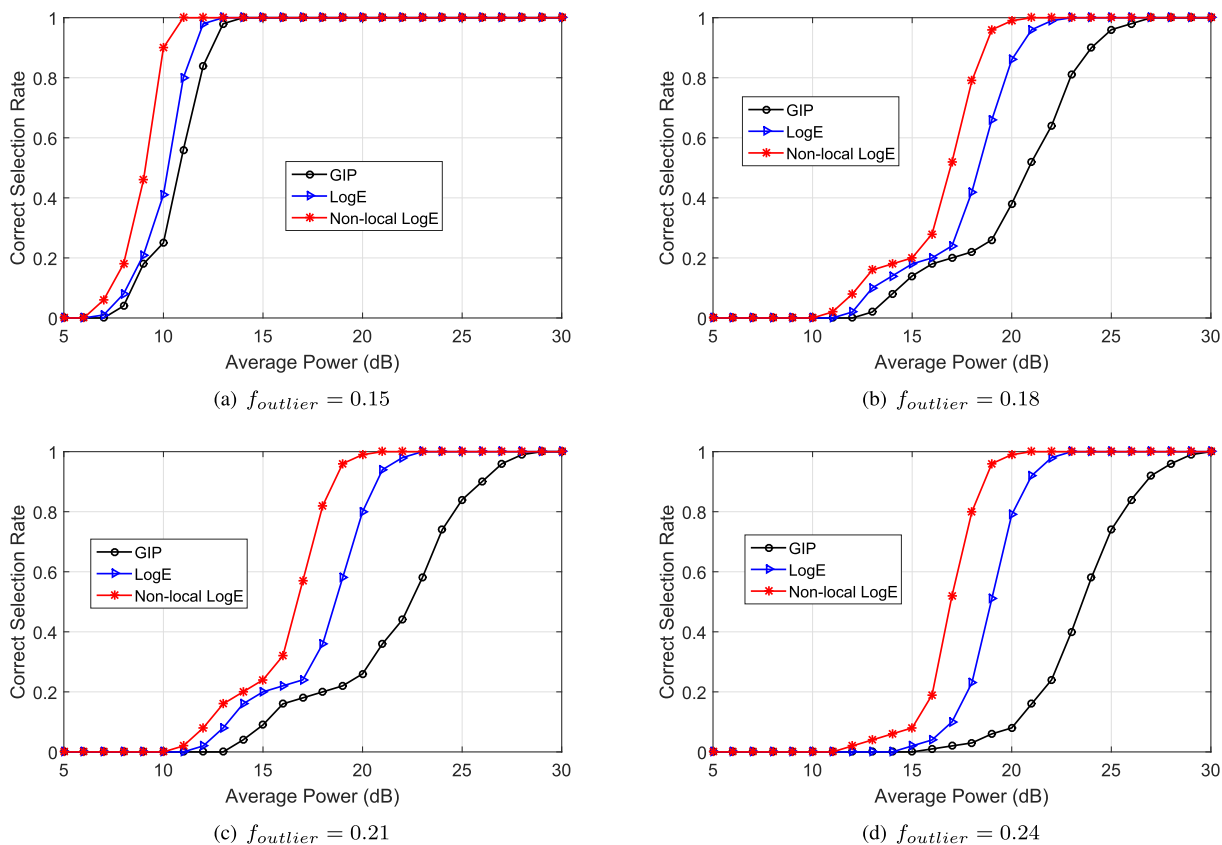


FIGURE 5. Illustrating the correct selection rate against average power from 5 dB to 30 dB with different normalized Doppler frequencies of outliers. $M = 100$, $N = 8$, $\sigma_c^2 = 15$ dB, $\rho = 0.92$, $N_{outlier} = 10$, $f = 0.25$.

in Section V-A, the robustness of the Log-Euclidean mean is better than that of the Euclidean mean. Then, the performance of the Log-Euclidean mean estimator is better than that of the Euclidean mean estimator in heterogeneous clutter when a sufficient number of secondary data is available. Therefore, the selection performance of the Log-Euclidean mean is better than that of the Euclidean mean. Moreover, as the non-local Log-Euclidean mean is obtained in the non-local domain, which discards the outlier priori to compute the Log-Euclidean mean. Thus, the selection performance of the non-local Log-Euclidean mean outperforms that of Log-Euclidean mean. Moreover, the selection performances of three selectors decrease, as the number of outlier increases. The result implies that the clutter environment becomes more nonhomogeneous with the increasing numbers of outliers, which result in a degradation in the selection performance.

In order to analyze the performance under different normalized Doppler frequencies of an outlier, a clutter environment is simulated, which has the same parameters except the normalized Doppler frequency of the outlier. The number of outlier is set to 10. The normalized Doppler frequencies of the outlier are set to be $f_o = 0.15$, $f_o = 0.18$, $f_o = 0.21$, and $f_o = 0.24$, respectively.

Figure 5 shows the correct selection rate against average power with different normalized Doppler frequencies of outliers. From Figure 5 we can know that different selector has

different performance at a certain outlier normalized Doppler frequency, and performances of selectors vary with different outlier normalized Doppler frequency. Specifically, the performance of the non-local Log-Euclidean selector outperforms that of the Log-Euclidean selector, followed by the GIP selector. The performance of the selector decreases and the performance difference among the three selectors increase, as the difference between the clutter normalized Doppler frequency and the outlier normalized Doppler frequency decreases. This is because the sample selector exploits the correlation to discriminate the outlier and the homogeneous sample data. As the closer the outlier Doppler is to the sample Doppler, the worse the correct selection rate will be.

C. APPLICATION OF TARGET DETECTION METHOD

Our proposed non-local Log-Euclidean mean-based sample selection algorithm is applied to target detection in real HF radar clutter. Sea clutter in HF radar often contains the first order and second order components. The first order clutter data is also known as Bragg lines caused by a resonant scattering of the transmitted radar signal, and the second order clutter comprises a few strong discrete scatters [27], [28]. The sea clutter data in HF radar often exhibits strong heterogeneity and need to be suppressed or eliminated [29]. The AMF algorithm is commonly used for target detection in sea clutter. An approximate theoretical value of the

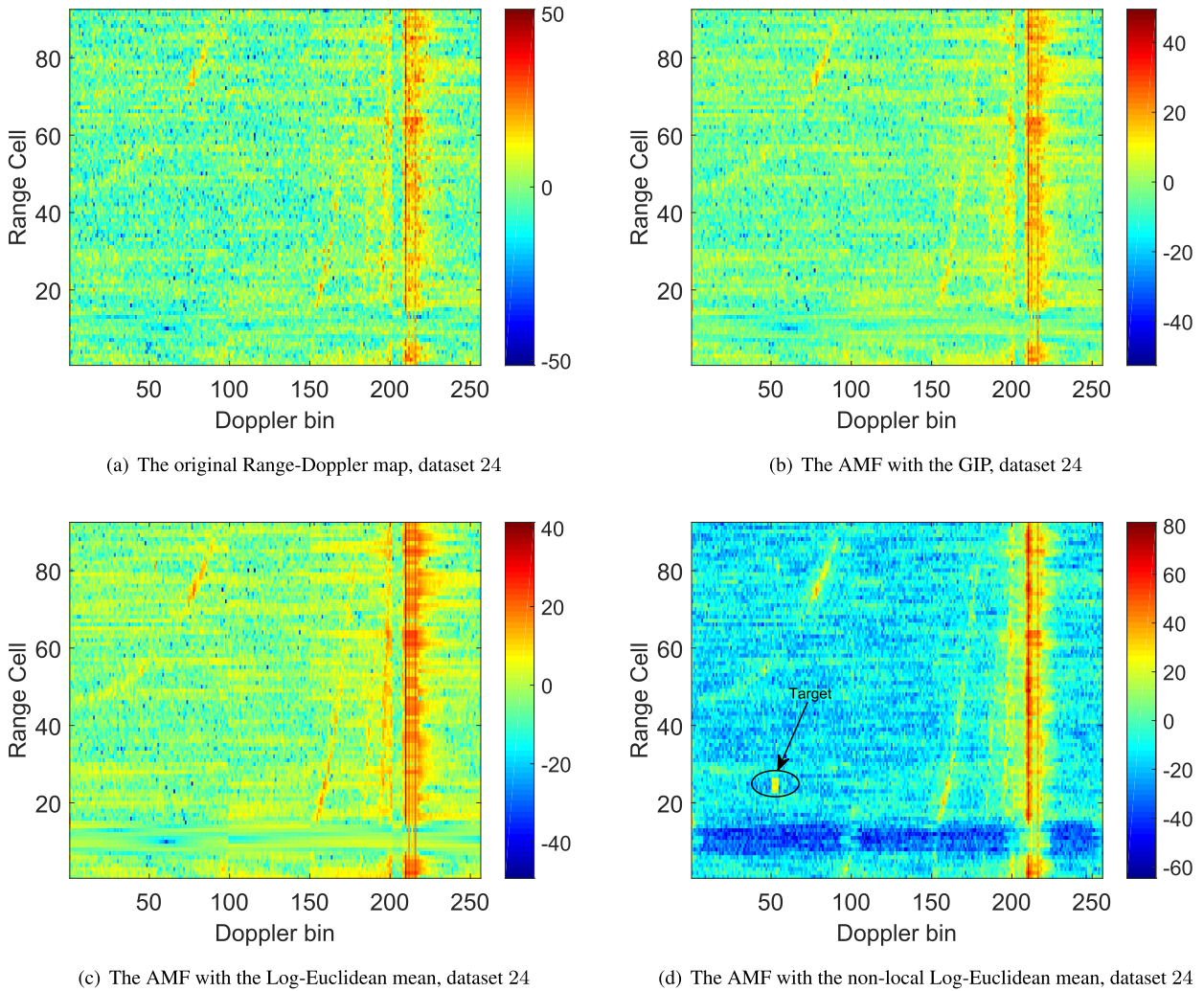


FIGURE 6. Illustrating the detection performance in real HF clutter dataset 24 with a simulated target. (a) The original Range-Doppler map, (b) Range-Doppler map of the GIP-based AMF algorithm, (c) Range-Doppler map of the Log-Euclidean mean-based AMF algorithm, (d) Range-Doppler map of the non-local Log-Euclidean mean-based AMF algorithm.

threshold has been given as eq. (24). This theoretical value is derived based on the compound-Gaussian model, which has been proven to be appropriate to describe the non-Gaussian radar clutter [30]. Many mostly used distributions, such as Gaussian, Log-normal, Weibull, K, Pareto, the generalized compound probability density function, can be modeled as a compound-Gaussian model. The detection algorithm in this paper contains the two parts, that are the sample selection part and the target detection part. The purpose of the sample selection part is to select the most homogeneous sample data. The selected sample data are seemed to be the homogeneous sample, which share the same spectral property, and conform to the same distribution. The target detection is conducted on these selected homogeneous sample data. Therefore, it is reasonable to use this theoretical value of the threshold to measure detection probability. As the performance of GIP sample selector is the worst among these three selectors, the detection performance of AMF with the GIP selector is also the worst. In this subsection, we analyze the detection performance of AMF with the non-local Log-Euclidean mean

in comparison with the Log-Euclidean mean. The real clutter data is collected by an HF system designed by Nanjing Institute of Technology in 2015. The number of receiving array is 16, and the sensor interval is 5m. The carrier frequency of the HF system is 15.82 MHz, and the pulse repetition frequency is 78.76 Hz.

A simulated target is injected into the batch 24 and 35 dataset, respectively. The target is located in the 23 ~ 26th range cells and 51 ~ 52th Doppler bins. The target signal is simulated as the model $\alpha \mathbf{p}$, where α accounts for the clutter power, \mathbf{p} is the target steering vector. The normalized Doppler frequency of the simulated target is 0.25 Hz. The SCR is defined as the ratio of the mean energy of target signal to the mean energy of clutter data surrounding the cell under test with 16 range-Doppler cells. The dataset contains 90 range cells, and 256 pulses data. $M = 64$ sample data is used for computing the Log-Euclidean mean. The size of the non-local domain is set to be $K = 32$. The detection performances of the AMF with the Log-Euclidean mean and the non-local Log-Euclidean mean are shown in Figure 6 and 7.

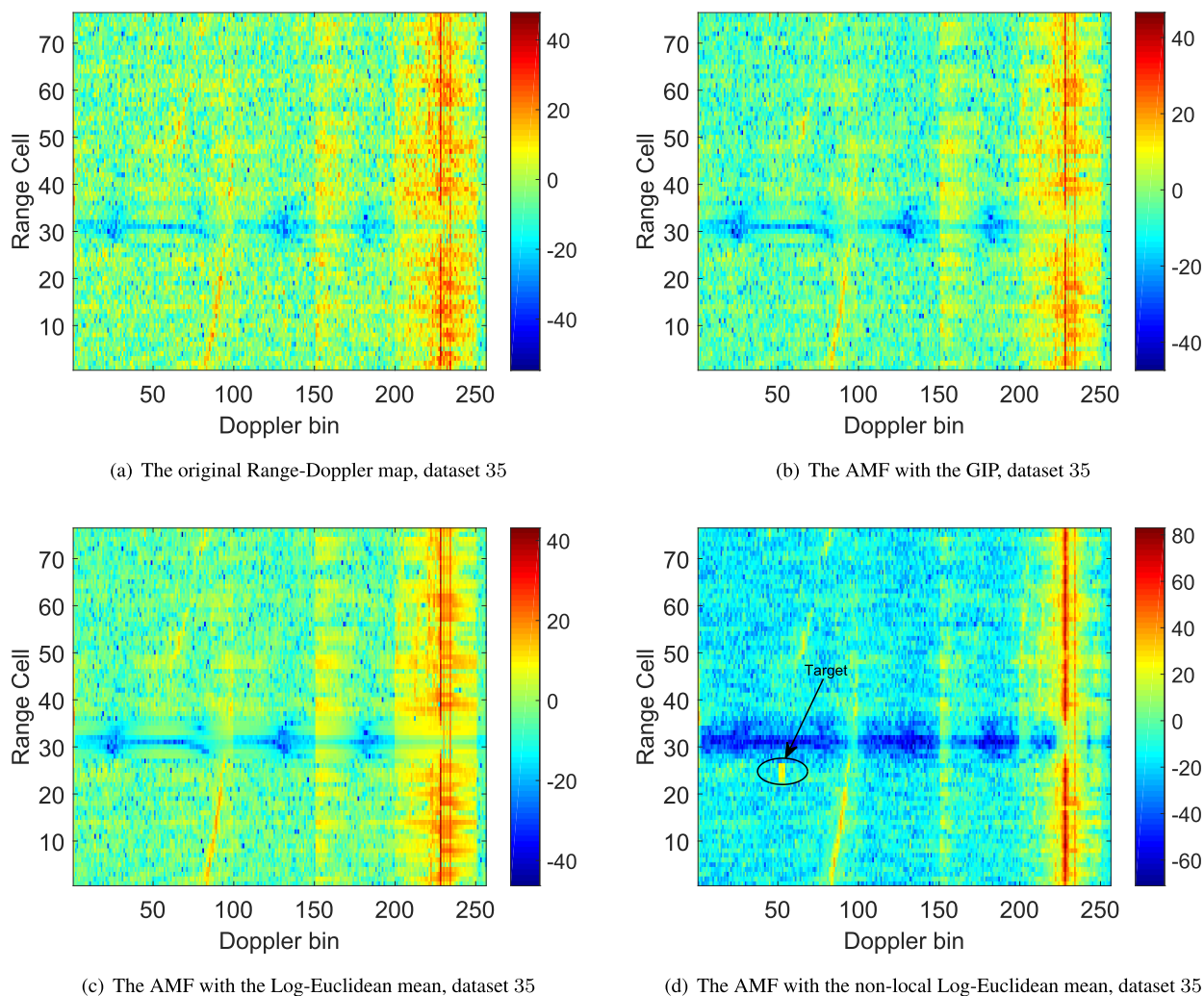


FIGURE 7. Illustrating the detection performance in real HF clutter dataset 35 with a simulated target. (a) The original Range-Doppler map, (b) Range-Doppler map of the GIP-based AMF algorithm, (c) Range-Doppler map of the Log-Euclidean mean-based AMF algorithm, (d) Range-Doppler map of the non-local Log-Euclidean mean-based AMF algorithm.

Figure 6 and 7 show the range-Doppler maps in dataset 24 and 35, respectively. Figure 6(c) and 7(c) are the range-Doppler maps of the Log-Euclidean mean-based AMF algorithm, and Figure 6(d) and 7(d) are the range-Doppler maps of our proposed detection algorithm.

The results show that the target can be detected by the non-local Log-Euclidean mean-based target detection algorithm. However, the target can not be detected by the Log-Euclidean mean-based AMF algorithm. In particular, the clutter power in the range-Doppler map of our proposed detection algorithm is lower than the range-Doppler map of Log-Euclidean mean-based AMF algorithm. It implies that the output signal-to-clutter rate (SCR) of our proposed detection algorithm is higher than that of the Log-Euclidean mean-based AMF algorithm. That is to say, our proposed algorithm can achieve a better clutter suppression performance with respect to the Log-Euclidean mean-based AMF algorithm. These results show the superiority of our proposed detection algorithm.

In order to compare detection performances of the AMF with the GIP (AMF-GIP), the AMF with the Log-Euclidean

mean (AMF-LEM), and the AMF with the non-local Log-Euclidean mean (NLLEM), three real HF sea clutter datasets (batch 24, 35, and 57) with a simulated target are used to estimate the detection probability (P_d) under different SCRs. Each dataset contains 90 range cells, and 256 Doppler bins. A simulated target is injected into the 45-th range cell. The 256 Doppler bins in each range cell are divided into 32 sample data. Each sample is modeled as an HPD matrix of order 8. The total 90 groups data are used for target detection, where each group includes 90 range cells and 8 Doppler bins. P_{ds} of the AMF-GIP, the AMF-LEM, and the AMF-NLLEM are estimated by the relative frequency of correct detection. The SCR varies from -10dB to 10dB . The probability of false alarm (P_{fa}) is set to be $P_{fa} = 10^{-5}$. Figure 8 shows the plot of P_{ds} of the AMF-GIP, the AMF-LEM, and the AMF-NLLEM under different SCRs in real HF sea clutter.

From Figure 8, it can be seen that our proposed algorithm has the best detection performance. In particular, the detection performance of the AMF-NLLEM is better than that of the AMF-LEM, which is followed by the AMF-GIP. This is because all three algorithms exploit AMF algorithm

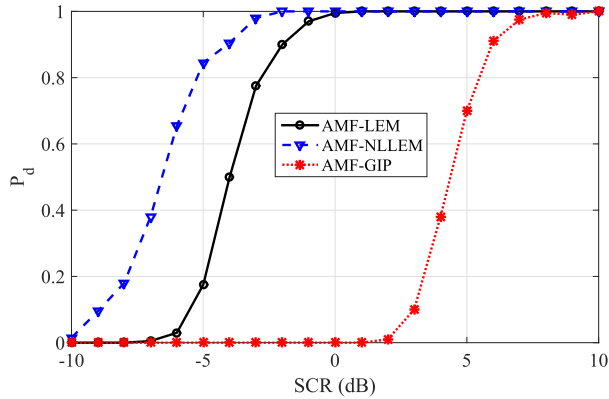


FIGURE 8. The plot of P_d vs SCRs in real HF sea clutter with a simulated target, $P_{fa} = 10^{-5}$.

to detection a moving target, and the essential difference between the three algorithms lies in different sample selectors. As performances of the three sample selectors are quite different, then, the homogeneity of the sample data used for target detection is different. Moreover, the performance of the non-local Log-Euclidean selector is much better than that of the GIP selector. Consequently, the detection performance of the AMF algorithm with the non-local Log-Euclidean mean is much better than that of the AMF algorithm with the GIP. These results can prove the superiority of detection performance of our proposed algorithm sufficiently.

VI. CONCLUSION

In this paper, we have presented a non-local Log-Euclidean mean-based algorithm for target detection in real HF nonhomogeneous clutter. In particular, we have proposed a non-local Log-Euclidean mean-based sample selection algorithm to choose the most homogeneous sample data. An adaptive matched filter with the non-local Log-Euclidean mean covariance estimator is used for target detection in the simulation and real HF nonhomogeneous clutter. At the analysis stage, we have analyzed the robustness of the Log-Euclidean mean and the Euclidean mean, and simulation experiments are given to assess the correct selection rates of the GIP, the GIP with the Log-Euclidean mean, and the GIP with non-local Log-Euclidean mean. Furthermore, we have assessed the detection performance in real HF sea clutter with a simulated target. These results have shown the superiority of our proposed algorithm.

APPENDIX

The Proof of Proposition 1: According to Eq.(10), let $F(\mathbf{P})$ be the objection function,

$$F(\mathbf{P}) = (1 - \varepsilon) \frac{1}{m} \sum_{i=1}^m \|\log(\mathbf{P}) - \log(\mathbf{P}_i)\|_F^2 + \varepsilon \frac{1}{n} \sum_{j=1}^n \|\log(\mathbf{P}) - \log(\mathbf{Q}_j)\|_F^2 \quad (25)$$

Note that $\tilde{\mathbf{P}}$ is the Log-Euclidean mean of m HPD matrices $\{\mathbf{P}_1, \mathbf{P}_2, \dots, \mathbf{P}_m\}$ and n outliers $\{\mathbf{Q}_1, \mathbf{Q}_2, \dots, \mathbf{Q}_n\}$, and we have

$$\begin{aligned} \tilde{\mathbf{P}} &= \arg \min_{\mathbf{P}} F(\mathbf{P}) \\ &\Rightarrow (1 - \varepsilon) \frac{1}{m} \sum_{i=1}^m 2(\log(\tilde{\mathbf{P}}) - \log(\mathbf{P}_i))\tilde{\mathbf{P}}^{-1} \\ &\quad + \varepsilon \frac{1}{n} \sum_{j=1}^n 2(\log(\tilde{\mathbf{P}}) - \log(\mathbf{Q}_j))\tilde{\mathbf{P}}^{-1} = 0 \\ &\Rightarrow (1 - \varepsilon) \frac{1}{m} \sum_{i=1}^m (\log(\tilde{\mathbf{P}}) - \log(\mathbf{P}_i)) \\ &\quad + \varepsilon \frac{1}{n} \sum_{j=1}^n (\log(\tilde{\mathbf{P}}) - \log(\mathbf{Q}_j)) = 0 \end{aligned} \quad (26)$$

$\bar{\mathbf{P}}$ is the Log-Euclidean mean of m HPD matrices $\{\mathbf{P}_1, \mathbf{P}_2, \dots, \mathbf{P}_m\}$, and we have,

$$\begin{aligned} \bar{\mathbf{P}} &= \arg \min_{\mathbf{P}} G(\mathbf{P}), G(\mathbf{P}) = \frac{1}{m} \sum_{i=1}^m \|\log(\bar{\mathbf{P}}) - \log(\mathbf{P}_i)\|_F^2 \\ &\Rightarrow \nabla G(\mathbf{P}) = \frac{1}{m} \sum_{i=1}^m 2(\log(\bar{\mathbf{P}}) - \log(\mathbf{P}_i))\bar{\mathbf{P}}^{-1} = 0 \\ &\Rightarrow \nabla G(\mathbf{P}) = \frac{1}{m} \sum_{i=1}^m (\log(\bar{\mathbf{P}}) - \log(\mathbf{P}_i)) = 0 \end{aligned} \quad (27)$$

Using the Taylor expansion on $\tilde{\mathbf{P}} = \bar{\mathbf{P}} + \varepsilon H(\mathbf{Q})$, and we can obtain,

$$\log(\tilde{\mathbf{P}}) = \log(\bar{\mathbf{P}}) + \varepsilon H(\mathbf{Q})\bar{\mathbf{P}}^{-1} \quad (28)$$

Substitute Eq. (28) into Eq.(26), and we have,

$$\begin{aligned} (1 - \varepsilon) \frac{1}{m} \sum_{i=1}^m (\log(\bar{\mathbf{P}}) + \varepsilon H(\mathbf{Q})\bar{\mathbf{P}}^{-1} - \log(\mathbf{P}_i)) \\ + \varepsilon \frac{1}{n} \sum_{j=1}^n (\log(\bar{\mathbf{P}}) + \varepsilon H(\mathbf{Q})\bar{\mathbf{P}}^{-1} - \log(\mathbf{Q}_j)) = 0 \\ \Rightarrow (1 - \varepsilon) \frac{1}{m} \sum_{i=1}^m (\log(\bar{\mathbf{P}}) - \log(\mathbf{P}_i)) + (1 - \varepsilon)\varepsilon H(\mathbf{Q})\bar{\mathbf{P}}^{-1} \\ + \varepsilon \frac{1}{n} \sum_{j=1}^n (\log(\bar{\mathbf{P}}) - \log(\mathbf{Q}_j)) + \varepsilon^2 H(\mathbf{Q})\bar{\mathbf{P}}^{-1} = 0 \end{aligned} \quad (29)$$

Consider Eq.(27) and Eq.(29), and ignore the terms contain ε^2 (as the term $\varepsilon \ll 1$),

$$\varepsilon H(\mathbf{Q})\bar{\mathbf{P}}^{-1} + \varepsilon \frac{1}{n} \sum_{j=1}^n (\log(\bar{\mathbf{P}}) - \log(\mathbf{Q}_j)) = 0 \quad (30)$$

Then, the influence function of Log-Euclidean mean can be given as follows,

$$H(\mathbf{Q}) = \frac{1}{n} \sum_{j=1}^n (\log(\mathbf{Q}_j) - \log(\bar{\mathbf{P}}))\bar{\mathbf{P}} \quad (31)$$

The Proof of Proposition 2: The mean $\bar{\mathbf{P}}$, associated with the Euclidean distance, of m HPD matrices $\{\mathbf{P}_1, \mathbf{P}_2, \dots, \mathbf{P}_m\}$ is the solution of the minimum as follow,

$$\bar{\mathbf{P}} = \underset{\mathbf{P} \in \mathbb{P}(n)}{\operatorname{argmin}} \frac{1}{m} \sum_{i=1}^m \|\mathbf{P} - \mathbf{P}_i\|_F^2 \quad (32)$$

Let $F(\mathbf{P})$ be the objection function,

$$F(\mathbf{P}) = (1 - \varepsilon) \frac{1}{m} \sum_{i=1}^m \|\mathbf{P} - \mathbf{P}_i\|_F^2 + \varepsilon \frac{1}{n} \sum_{j=1}^n \|\mathbf{P} - \mathbf{Q}_j\|_F^2 \quad (33)$$

The derivative of objection function $F(\mathbf{P})$ is,

$$\nabla F(\mathbf{P}) = (1 - \varepsilon) \frac{1}{m} \sum_{i=1}^m 2(\mathbf{P} - \mathbf{P}_i) + \varepsilon \frac{1}{n} \sum_{j=1}^n 2(\mathbf{P} - \mathbf{Q}_j) \quad (34)$$

$\tilde{\mathbf{P}}$ is the Euclidean mean of m HPD matrices $\{\mathbf{P}_1, \mathbf{P}_2, \dots, \mathbf{P}_m\}$ and n outliers $\{\mathbf{Q}_1, \mathbf{Q}_2, \dots, \mathbf{Q}_n\}$, and we have

$$\begin{aligned} \tilde{\mathbf{P}} &= \underset{\mathbf{P}}{\operatorname{argmin}} F(\mathbf{P}) \\ \Rightarrow \nabla F(\tilde{\mathbf{P}}) &= (1 - \varepsilon) \frac{1}{m} \sum_{i=1}^m 2(\tilde{\mathbf{P}} - \mathbf{P}_i) \\ &\quad + \varepsilon \frac{1}{n} \sum_{j=1}^n 2(\tilde{\mathbf{P}} - \mathbf{Q}_j) = 0 \end{aligned} \quad (35)$$

$\bar{\mathbf{P}}$ is the Euclidean mean of m HPD matrices $\{\mathbf{P}_1, \mathbf{P}_2, \dots, \mathbf{P}_m\}$, and $\bar{\mathbf{P}}$ can be given,

$$\begin{aligned} \bar{\mathbf{P}} &= \underset{\mathbf{P}}{\operatorname{argmin}} G(\mathbf{P}), G(\mathbf{P}) = \frac{1}{m} \sum_{i=1}^m \|\mathbf{P} - \mathbf{P}_i\|_F^2 \\ \Rightarrow \nabla F(\bar{\mathbf{P}}) &= \frac{1}{m} \sum_{i=1}^m 2(\bar{\mathbf{P}} - \mathbf{P}_i) = 0 \end{aligned} \quad (36)$$

Substitute $\tilde{\mathbf{P}} = \bar{\mathbf{P}} + \varepsilon H(\mathbf{Q})$ into Eq.(35), and we have,

$$\begin{aligned} 2(1 - \varepsilon) \frac{1}{m} \sum_{i=1}^m (\bar{\mathbf{P}} + \varepsilon H(\mathbf{Q}) - \mathbf{P}_i) \\ + 2\varepsilon \frac{1}{n} \sum_{j=1}^n (\bar{\mathbf{P}} + \varepsilon H(\mathbf{Q}) - \mathbf{Q}_j) &= 0 \\ \Rightarrow (1 - \varepsilon) \frac{1}{m} \sum_{i=1}^m (\bar{\mathbf{P}} - \mathbf{P}_i) + (1 - \varepsilon)\varepsilon H(\mathbf{Q}) \\ + \varepsilon \frac{1}{n} \sum_{j=1}^n (\bar{\mathbf{P}} + \varepsilon H(\mathbf{Q}) - \mathbf{Q}_j) &= 0 \\ \Rightarrow \varepsilon H(\mathbf{Q}) - \varepsilon^2 H(\mathbf{Q}) + \varepsilon \frac{1}{n} \sum_{j=1}^n (\bar{\mathbf{P}} - \mathbf{Q}_j) + \varepsilon^2 H(\mathbf{Q}) &= 0 \end{aligned} \quad (37)$$

Consider Eq.(36) and Eq.(37), and ignore the terms contain ε^2 . Then, the influence function of Euclidean mean

can be formulated as,

$$H(\mathbf{Q}) = \frac{1}{n} \sum_{j=1}^n (\mathbf{Q}_j - \bar{\mathbf{P}}) \quad (38)$$

In the following, we give the proof of the appropriate threshold.

The probability of false alarm (P_{fa}) has an integral form,

$$P_{fa} = \int_0^1 P_{fa|\rho} f(\rho) d\rho \quad (39)$$

where

$$f(\rho) = \frac{K!}{(N-2)!(K-N+1)!} (1-\rho)^{N-2} \rho^{K-N+1} \quad (40)$$

and

$$P_{fa|\rho} = (1 + \rho\gamma)^{-(K-N+1)} \quad (41)$$

Substitute Eq.(40) and Eq.(41) into Eq.(39), and then, we have [31]

$$\begin{aligned} P_{fa} &= \frac{K!}{(N-2)!(K-N+1)!} \int_0^1 \rho^{(K-N+1)} \\ &\quad \times (1-\rho)^{(N-2)} (1+\rho\gamma)^{-(K-N+1)} d\rho \\ &= F_1^2(K-N+1, K_N+2; K+1; -\gamma) \end{aligned} \quad (42)$$

where $F_1^2(a, b; c; x)$ is the Gaussian hypergeometric function, which is defined as [31],

$$F_1^2(a, b; c; x) = \sum_{i=0}^{\infty} \frac{(a)_i (b)_i}{(c)_i i!} x^i \quad (43)$$

with the Pochhammer symbol $(a)_i = a(a+1)\dots(a+i-1)$. According to the Theorem of [31], Eq.(42) can be formulated as a Gaussian hypergeometric function

$$\begin{aligned} P_{fa} &= G(K-N+1, K_N+2; K+1; -\gamma) \\ &= \left(1 + \frac{K-N+1}{K+1} \gamma\right)^{-(K-N+2)} \end{aligned} \quad (44)$$

Thus, the threshold γ can be given as

$$\gamma = \frac{K+1}{K-N+1} [(P_{fa})^{(-\frac{1}{K-N+2})} - 1] \quad (45)$$

ACKNOWLEDGMENT

The authors are grateful for the valuable comments made by the reviewers, which have assisted us with a better understanding of the underlying issues and therefore a significant improvement in the quality of the paper.

REFERENCES

- [1] F. Jangal, S. Saillant, and M. Helier, "Wavelet contribution to remote sensing of the sea and target detection for a high-frequency surface wave radar," *IEEE Geosci. Remote Sens. Lett.*, vol. 5, no. 3, pp. 552-556, Jul. 2008.
- [2] J.-M. Le Caillec, T. Górski, G. Sicot, and A. Kawalec, "Theoretical performance of space-time adaptive processing for ship detection by high-frequency surface wave radars," *IEEE J. Ocean. Eng.*, vol. 43, no. 1, pp. 238-257, Jan. 2018.

- [3] A. Dzvonkovskaya, K. Gurgel, H. Rohling, and T. Schlick, "Low power high frequency surface wave radar application for ship detection and tracking," in *Proc. Int. Conf. Radar*, Sep. 2008, pp. 627–632.
- [4] S. Grosdidier and A. Baussard, "Ship detection based on morphological component analysis of high-frequency surface wave radar images," *IET Radar, Sonar Navigat.*, vol. 6, no. 9, pp. 813–821, Dec. 2012.
- [5] E. J. Kelly, "An adaptive detection algorithm," *IEEE Trans. Aerosp. Electron. Syst.*, vol. AES-22, no. 2, pp. 115–127, Mar. 1986.
- [6] F. C. Robey, D. R. Fuhrmann, E. J. Kelly, and R. Nitzberg, "A CFAR adaptive matched filter detector," *IEEE Trans. Aerosp. Electron. Syst.*, vol. 28, no. 1, pp. 208–216, Jan. 1992.
- [7] E. Conte, M. Lops, and G. Ricci, "Adaptive detection schemes in compound-Gaussian clutter," *IEEE Trans. Aerosp. Electron. Syst.*, vol. 34, no. 4, pp. 1058–1069, Oct. 1998.
- [8] A. De Maio, A. Farina, and G. Foglia, "Design and experimental validation of knowledge-based constant false alarm rate detectors," *IET Radar, Sonar Navigat.*, vol. 1, no. 4, pp. 308–316, Aug. 2007.
- [9] A. De Maio, A. Farina, and G. Foglia, "Knowledge-aided Bayesian radar detectors & their application to live data," *IEEE Trans. Aerosp. Electron. Syst.*, vol. 46, no. 1, pp. 170–183, Jan. 2010.
- [10] A. Aubry, V. Carotenuto, A. De Maio, and G. Foglia, "Exploiting multiple a priori spectral models for adaptive radar detection," *IET Radar, Sonar Navigat.*, vol. 8, no. 7, pp. 695–707, Aug. 2014.
- [11] P. Wang, H. Li, and B. Himed, "Knowledge-aided parametric tests for multichannel adaptive signal detection," *IEEE Trans. Signal Process.*, vol. 59, no. 12, pp. 5970–5982, Dec. 2011.
- [12] H. Li and J. H. Michels, "Parametric adaptive signal detection for hyperspectral imaging," *IEEE Trans. Signal Process.*, vol. 54, no. 7, pp. 2704–2715, Jul. 2006.
- [13] A. Wiesel, O. Bibi, and A. Globerson, "Time varying autoregressive moving average models for covariance estimation," *IEEE Trans. Signal Process.*, vol. 61, no. 11, pp. 2791–2801, Jun. 2013.
- [14] A. De Maio, D. Orlando, C. Hao, and G. Foglia, "Adaptive detection of point-like targets in spectrally symmetric interference," *IEEE Trans. Signal Process.*, vol. 64, no. 12, pp. 3207–3220, Jun. 2016.
- [15] G. Foglia, C. Hao, A. Farina, G. Giunta, D. Orlando, and C. Hou, "Adaptive detection of point-like targets in partially homogeneous clutter with symmetric spectrum," *IEEE Trans. Aerosp. Electron. Syst.*, vol. 53, no. 4, pp. 2110–2119, Aug. 2017.
- [16] J. Lapuyade-Lahorgue and F. Barbaresco, "Radar detection using Siegel distance between autoregressive processes, application to HF and X-band radar," in *Proc. IEEE Radar Conf.*, May 2008, pp. 1–6.
- [17] F. Barbaresco, "Innovative tools for radar signal processing based on Cartan's geometry of SPD matrices & information geometry," in *Proc. IEEE Radar Conf.*, May 2008, pp. 1–6.
- [18] X. Hua, Y. Cheng, H. Wang, Y. Qin, Y. Li, and W. Zhang, "Matrix CFAR detectors based on symmetrized Kullback–Leibler and total Kullback–Leibler divergences," *Digit. Signal Process.*, vol. 69, pp. 106–116, Oct. 2017.
- [19] X. Hua, Y. Cheng, H. Wang, Y. Qin, and Y. Li, "Geometric means and medians with applications to target detection," *IET Signal Process.*, vol. 11, no. 6, pp. 711–720, 2017.
- [20] Z. Liu and F. Barbaresco, "Doppler information geometry for wake turbulence monitoring," in *Matrix Information Geometry*. Berlin, Germany: Springer, 2013, pp. 277–290.
- [21] F. Barbaresco and U. Meier, "Radar monitoring of a wake vortex: Electromagnetic reflection of wake turbulence in clear air," *Comp. Rendus Phys.*, vol. 11, no. 1, pp. 54–67, 2010.
- [22] F. Barbaresco, "Robust statistical radar processing in Fréchet metric space: OS-HDR-CFAR and OS-STAP processing in Siegel homogeneous bounded domains," in *Proc. 12th Int. Radar Symp. (IRS)*, Sep. 2011, pp. 639–644.
- [23] B. Balaji and F. Barbaresco, "Riemannian mean and space-time adaptive processing using projection and inversion algorithms," *Proc. SPIE*, vol. 8714, May 2013, Art. no. 871419.
- [24] X. Hua, Y. Cheng, H. Wang, and Y. Qin, "Robust covariance estimators based on information divergences and Riemannian manifold," *Entropy*, vol. 20, no. 4, p. 219, 2018. [Online]. Available: <http://www.mdpi.com/1099-4300/20/4/219>
- [25] A. Aubry, A. D. Maio, L. Pallotta, and A. Farina, "Covariance matrix estimation via geometric barycenters and its application to radar training data selection," *IET Radar, Sonar Navigat.*, vol. 7, no. 6, pp. 600–614, Jul. 2013.
- [26] G. Cui, N. Li, L. Pallotta, G. Foglia, and L. Kong, "Geometric barycenters for covariance estimation in compound-Gaussian clutter," *IET Radar, Sonar Navigat.*, vol. 11, no. 3, pp. 404–409, 2017.
- [27] H. Leong, "Dependence of HF surface wave radar sea clutter on sea state," in *Proc. RADAR*, Oct. 2002, pp. 56–60.
- [28] A. Bourdillon, P. Dorey, and G. Auffray, "Ship echo discrimination in HF radar sea-clutter," in *Proc. Int. Conf. Radar*, Sep. 2003, pp. 584–587.
- [29] A. Gupta and T. Fickenscher, "Sea clutter canceller for shipborne HF surface wave radar," in *Proc. Int. ITG Workshop Smart Antennas*, Feb. 2011, pp. 1–4.
- [30] L. P. Roy and R. V. R. Kumar, "A GLRT detector in partially correlated texture based compound-Gaussian clutter," in *Proc. Nat. Conf. Commun. (NCC)*, Jan. 2010, pp. 1–5.
- [31] J. Liu, H. Li, and B. Himed, "Threshold setting for adaptive matched filter and adaptive coherence estimator," *IEEE Signal Process. Lett.*, vol. 22, no. 1, pp. 11–15, Jan. 2015.



WEI CHEN received the M.Sc. degree from Fudan University, in 2008. He is currently an Associate Professor and a Master's Supervisor with the Industrial Center, Nanjing Institute of Technology. He is also the Head of the Ministry of Intelligence, Shenzhen Kuang-Chi Space Technology Company, Ltd. His research fields focus on intelligent robots and image processing.



SIYU CHEN is currently pursuing the master's degree with the Department of Electrical and Computer Engineering, Technical University of Munich, Germany. Her research fields focus on intelligent robots and image processing.

...